

Two-dimensional easy-plane SU(3) magnet with the transverse field: Anisotropy-driven multicriticality

Yoshihiro Nishiyama

Department of Physics, Faculty of Science, Okayama University, Okayama 700-8530, Japan

Abstract. The two-dimensional easy-plane SU(3) magnet subjected to the transverse field was investigated with the exact-diagonalization method. So far, as to the XY model (namely, the easy-plane SU(2) magnet), the transverse-field-driven order-disorder phase boundary has been investigated with the exact-diagonalization method, and it was claimed that the end-point singularity (multicriticality) at the XX -symmetric point does not accord with large- N -theory's prediction. Aiming to reconcile the discrepancy, we extend the internal symmetry to the easy-plane SU(3) with the anisotropy parameter η , which interpolates the isotropic ($\eta = 0$) and fully anisotropic ($\eta = 1$) cases smoothly. As a preliminary survey, setting $\eta = 1$, we analyze the order-disorder phase transition through resorting to the fidelity susceptibility χ_F , which exhibits a pronounced signature for the criticality. Thereby, with η scaled carefully, the χ_F data are cast into the crossover-scaling formula so as to determine the crossover exponent ϕ , which seems to reflect the extension of the internal symmetry group to SU(3).

1. Introduction

The one-dimensional XY model subjected to the transverse field H and anisotropy η with the Hamiltonian $\mathcal{H}_{XY} = -\sum_i [(1 + \eta)\sigma_i^x \sigma_{i+1}^x + (1 - \eta)\sigma_i^y \sigma_{i+1}^y + H\sigma_i^z]$ (σ_i : Pauli matrices at site i) is attracting much attention [1, 2, 3, 4] in the context of the quantum information theory [5, 6]. A key ingredient is that the model covers both XX - ($\eta = 0$) and Ising-symmetric ($\eta = 1$) cases, and there appear rich characters as to the transverse-field-driven order-disorder phase transition. Recently, the multicriticality at $\eta = 0$, *i.e.*, the end-point singularity of the phase boundary toward the XX -symmetric point, was explored in depth from the quantum-information-theoretical viewpoint [7].

Meanwhile, its extension to the two-dimensional counterpart has been made [8, 9]. According to the large- N theory [9], namely, for sufficiently large internal symmetry group, the phase boundary should exhibit a reentrant (non-monotonic) behavior. The reentrant behavior leads to a counterintuitive picture such that the disorder phase is induced by the lower internal symmetry group. On the contrary, as to the XY (namely, easy-plane SU(2)) model, the exact-diagonalization study [8, 9, 10] claimed that the phase boundary rises up linearly (monotonically) in proximity to the multicritical point;

the similar phase diagram was reported in Ref. [11], where a topological index is specified to each phase surrounding the multicritical point. Rather technically, it has to be stressed that the exact-diagonalization method allows direct access to the ground state (namely, infinite imaginary-time system size), and hence, we do not have to care about the anisotropy between the real-space and imaginary-time directions rendered by the dynamical critical exponent $z = 2 (\neq 1)$ [12] at the multicritical point.

The aim of this paper is to reconcile the discrepancy between the large- N - [9] and easy-plane-SU(2)-based [8, 9, 10] results; namely, so far, only the extremum cases have been considered. For that purpose, we extend the internal symmetry group to the easy-plane SU(3) [13], and explore how the extension of the internal symmetry group affects the multicriticality. Additionally, as a probe to detect the phase transition [14, 15, 16, 17, 18, 19, 20, 21], we resort to the fidelity [22, 23, 24, 25]

$$F(H, H + \Delta H) = |\langle H | H + \Delta H \rangle|, \quad (1)$$

where the vectors, $|H\rangle$ and $|H + \Delta H\rangle$, denote the ground states with the proximate interaction parameters, H and $H + \Delta H$, respectively. The fidelity (1) is readily accessible via the exact-diagonalization method, which yields the ground-state vector $|H\rangle$ explicitly. According to the elaborated exact-diagonalization study of the two-dimensional XXZ and Ising models [17], the fidelity-mediated analysis admits a reliable estimate for the criticality, although the available system size $N \leq 20$ is rather restricted.

To be specific, we present the Hamiltonian for the two-dimensional easy-plane SU(3) magnet subjected to the transverse field

$$\mathcal{H} = -J \sum_{\langle ij \rangle} [(1+\eta)(S_i^x S_j^x + S_i^y S_j^y) + (1-\eta)(Q_i^{zx} Q_j^{zx} + Q_i^{yz} Q_j^{yz})] + H \sum_{i=1}^N Q_i^{z^2}, \quad (2)$$

with the $S = 1$ -spin operator \mathbf{S}_i placed at each square-lattice point $i = 1, 2, \dots, N$. Likewise, the quadrupolar moments at site i , $Q_i^{x^2-y^2} = (S_i^x)^2 - (S_i^y)^2$, $Q_i^{z^2} = \sqrt{3}(S_i^z)^2 - \frac{2}{\sqrt{3}}$, $Q_i^{xy} = S_i^x S_i^y + S_i^y S_i^x$, $Q_i^{yz} = S_i^y S_i^z + S_i^z S_i^y$, and $Q_i^{zx} = S_i^z S_i^x + S_i^x S_i^z$, are incorporated. These eight operators constitute the SU(3) algebra [26] just like the Gell-Mann matrices. The summation $\sum_{\langle ij \rangle}$ runs over all possible nearest-neighbor pairs $\langle ij \rangle$, and the coupling constant J sets the unit of energy, $J = 1$, throughout this study. The parameters, η and H , denote the anisotropy of the internal symmetry and the transverse field, respectively. The anisotropy $\eta \neq 0$ gives rise to the asymmetry between the $S_i^{x,y}$ and $Q_i^{yz,zx}$ sectors. Irrespective of the anisotropy η , the Hamiltonian commutes with the z -axis-rotation generator $\sum_{i=1}^N S_i^z$, and hence, the Hamiltonian (2) describes the easy-plane sector of the SU(3) magnet.

In Fig. 1, we present a schematic phase diagram of the easy-plane SU(3) magnet (2) for the anisotropy η and the transverse field H ; the overall character would resemble that of the XY model [8]. The phase boundary $H_c(\eta)$ separates the order ($H < H_c(\eta)$) and disorder ($H > H_c(\eta)$) phases. In the order phase, there appears the spontaneous magnetization of the in-plane moment (S_i^x, S_i^y) [(Q_i^{zx}, Q_i^{yz})] for the $\eta > (<)0$ regime. Therefore, the phase boundary $H = H_c(\eta)$ should belong to the three-dimensional (3D) XY universality class *except* at the multicritical point $\eta = 0$. At $\eta = 0$, the Hamiltonian

(2) commutes with the transverse moment $\sum_{i=1}^N Q_i^{z^2}$. Hence, as the transverse field H increases, the successive level crossings take place as to the ground-state energy up to $H < H_c(0) (= 8/\sqrt{3})$ [7], and above the threshold $H > H_c(0)$, the transverse moment $\sum_{i=1}^N Q_i^{z^2}$ saturates eventually; see Appendix. This transition mechanism is the same as that of the magnetization plateau (saturation of magnetization), and the power-law singularities have been investigated in depth [12]. Around the threshold $H = H_c(0)$, the efficiency of the quantum Monte Carlo sampling suffers from the slowing-down problem [27], and the aforementioned exact-diagonalization study [8] circumvented this difficulty.

Then, there arises a problem how the phase boundary $H_c(\eta)$ terminates at the multicritical point $\eta = 0$; see Fig. 2. The exact-diagonalization analysis of the XY model indicates that the phase boundary $H_c(\eta)$ rises up linearly (monotonically) [8, 9] around the multicritical point $\eta = 0$. Actually, the power-law singularity of the phase boundary [28, 29]

$$H_c(\eta) - H_c(0) \sim |\eta|^{1/\phi}, \quad (3)$$

is characterized by the crossover exponent $\phi \approx 1$ as for the XY magnet [8, 9, 10]. On the one hand, the large- N theory [9] suggests that the phase boundary $H_c(\eta)$ shows a reentrant behavior. That is, the phase boundary $H_c(\eta)$ exhibits a non-monotonic dependence on the anisotropy η . So far, only the limiting cases such as the XY [8, 9, 10] and spherical [9] models have been considered, and no information has been provided as to the multicriticality in between. As the internal symmetry group is enlarged gradually from SU(2), the phase boundary may become curved convexly, accompanying with the suppressed crossover exponent $\phi < 1$. In this paper, considering the SU(3) version of the easy-plane magnet, we investigate the crossover exponent ϕ quantitatively by the agency of the fidelity $F(H, H + \Delta H)$ (1).

The rest of this paper is organized as follows. In Sec. 2, we present the numerical results. Prior to the detailed analysis of the multicriticality, we investigate the case of the fully anisotropic limit $\eta = 1$, aiming to demonstrate the performance of our simulation scheme. In the last section, we address the summary and discussions.

2. Numerical results

In this section, we present the numerical results for the easy-plane SU(3) magnet subjected to the transverse field (2). We employed the exact-diagonalization method for the finite-size cluster with $N \leq 5 \times 5$ spins. The linear dimension of the cluster is given by $L = \sqrt{N}$, which sets the fundamental length scale in the subsequent finite-size-scaling analyses. As a probe to detect the phase transition, we utilized the fidelity susceptibility [14, 15, 16, 17, 18, 19, 20, 21]

$$\chi_F(H) = -\frac{1}{L^2} \partial_{\Delta H}^2 F(H, H + \Delta H)|_{\Delta H=0}, \quad (4)$$

with the fidelity $F(H, H + \Delta H)$ (1). As was demonstrated in Ref. [17] for the two-dimensional XXZ and Ising models under the transverse field with $N \leq 20$ spins, the

fidelity susceptibility χ_F (4) admits a reliable estimate of the criticality, even though the available system size $N \leq 20$ is rather restricted.

In fairness, it has to be mentioned that the similar scheme was applied to the *one-dimensional XY* magnet under the transverse field [7]. In this pioneering study [7], the authors took a direct route toward the multicritical point, $(\eta, H) \rightarrow (0, H_c(0))$. The χ_F data exhibit the intermittent peaks, reflecting the successive level crossings along the ordinate axis $\eta = 0$, as shown in Fig. 1. In this paper, to avoid such a finite-size artifact, we took a different route to the multicritical point, keeping the anisotropy η to a finite value. That is, based on the crossover-scaling theory [28, 29], the anisotropy η is scaled properly, as the system size L changes. As a byproduct, we are able to estimate the crossover exponent ϕ quantitatively, which characterizes the power-law singularity of the phase boundary; see Fig. 2. Before commencing detailed crossover-scaling analyses of χ_F , we devote ourselves to the fully anisotropic case $\eta = 1$ so as to examine the performance of our simulation scheme.

2.1. Phase transition point $H_c(1)$ at $\eta = 1$: Fidelity-susceptibility analysis

In this section, as a preliminary survey, setting the anisotropy parameter to the fully anisotropic limit $\eta = 1$, we investigate the order-disorder phase transition of the easy-plane SU(3) magnet under the transverse field (2) via the fidelity susceptibility χ_F (4). At this point $\eta = 1$, the model (2) reduces to the spin- $S = 1$ XY model with the single-ion anisotropy D , for which a variety of preceding results are available [30, 31, 32, 33, 34, 35].

In Fig. 3, we present the fidelity susceptibility χ_F (4) for various values of the transverse field H , and the system sizes, (+) $L = 3$, (\times) 4, and (*) 5, with the fixed $\eta = 1$. We see that the fidelity susceptibility exhibits a pronounced signature for the order-disorder phase transition around $H \approx 6$.

In Fig. 4, we present the approximate critical point $H_c^*(L)$ for $1/L^{1/\nu}$ with $\eta = 1$ fixed. Here, the approximate critical point $H_c^*(L)$ denotes the location of the fidelity-susceptibility peak

$$\partial_H \chi_F(L)|_{H=H_c^*(L)} = 0, \tag{5}$$

for each system size L . The power of the abscissa scale $1/\nu$ comes from the scaling dimension of the parameter H [20], and the correlation-length critical exponent ν is set to the value of the 3D-XY universality class, $\nu = 0.6717$ [36, 37]; the validity of this proposition is examined in the next section. From Fig. 4, the least-squares fit to these data yields an estimate

$$H_c(\eta = 1) = 6.53(5), \tag{6}$$

in the thermodynamic limit $L \rightarrow \infty$.

This is a good position to address an overview of the related studies. In Table 1, we recollect a number of preceding results for the critical point $H_c(1)$ at the fully anisotropic case $\eta = 1$. As mentioned above, at $\eta = 1$, our model (2) reduces to the

spin- $S = 1$ XY model with the single-ion anisotropy D , and the D -based results are converted via the relation $H = 2D/\sqrt{3}$ so as to match our notation. As shown in table 1, the critical point $H_c(1)$ was estimated as $H_c = 6.300$ [30], 6.628 [31, 32], and 6.524(23) [33] by means of the bosonic mean-field approximation (BMFA), self-consistent harmonic approximation (SCHA), and quantum Monte Carlo (QMC) methods, respectively. (The BMFA estimate is read off from Fig. 1 of Ref. [30].) As a probe to detect the phase transition, various quantifiers, such as the spontaneous magnetization, energy gap, and correlation length, were utilized in the respective studies. As indicated, we also incorporated the Heisenberg-model [34, 35] result [33], because “the anisotropy does not have large effects” [30] as to the critical point H_c . Our exact-diagonalization (ED) result $H_c = 6.53(5)$ [Eq. (6)] obtained via the fidelity susceptibility χ_F appears to be accordant with these preceding studies. Particularly, our result $H_c = 6.53(5)$ [Eq. (6)] agrees with the large-scale-QMC-simulation result 6.524(23) [33], validating the χ_F -mediated simulation scheme. Encouraged by this finding, we further explore the critical behavior of χ_F in the next section.

2.2. Criticality of the fidelity susceptibility at $\eta = 1$

In this section, we investigate the criticality of the fidelity susceptibility χ_F (4) at the fully anisotropic limit, $\eta = 1$. To begin with, we set up the finite-size-scaling formula for the fidelity susceptibility [20]

$$\chi_F = L^{\alpha_F/\nu} f\left((H - H_c)L^{1/\nu}\right), \quad (7)$$

with a scaling function f , and the fidelity-susceptibility critical exponent α_F ; namely, the index α_F describes the singularity $\chi_F \sim |H - H_c|^{-\alpha_F}$ at the critical point H_c . According to Ref. [20], the critical exponent α_F satisfies the relation

$$\alpha_F/\nu = \alpha/\nu + 1, \quad (8)$$

with the specific-heat critical index α ; namely, the index α describes the singularity of the specific heat as $C \sim |H - H_c|^{-\alpha}$. We postulate that the the criticality belongs to the 3D- XY universality class [36, 37] for the anisotropic regime $\eta \neq 0$. Putting the existing values [36], $\alpha = 0.0151$ and $\nu = 0.6717$, for the 3D- XY universality class into the scaling relation (8), we arrive at

$$\alpha_F/\nu = 0.9775. \quad (9)$$

Notably, this index $\alpha_F/\nu = 0.9775$ is larger than that of the specific heat, $\alpha/\nu = -0.0225$ [36]; actually, the latter takes a negative value. The scaling parameters, α_F/ν and ν , appearing in the expression (7) are all fixed, and we are able to carry out the scaling analysis of χ_F unambiguously.

In Fig. 5 we present the scaling plot, $(H - H_c)L^{1/\nu}\chi_FL^{-\alpha_F/\nu}$, for various H and system sizes, (+) $L = 3$, (\times) 4, and (*) 5, with the fixed $\eta = 1$. Here, the scaling parameters are set to $H_c = 6.53$ [Eq. (6)], $\nu = 0.6717$ [36], and $\alpha_F/\nu = 0.9775$ [Eq. (9)]. The scaled data appear to collapse into the scaling curve satisfactorily, confirming

that the simulation data already enter into the scaling regime. We stress that no *ad hoc* parameter adjustment is undertaken in the present scaling analysis.

We address a number of remarks. First, the scaling plot, Fig. 5, indicates that the phase transition belongs to the 3D- XY universality class. So far, as for the *Heisenberg antiferromagnet* with the single-ion anisotropy D , it has been claimed that the D -driven singularity belongs to the 3D- XY universality class [33, 35]. Our simulation result shows that the quantum XY ferromagnet is also under the reign of the 3D- XY universality class. Second, from the scaling plot, Fig. 5, we see that corrections to finite-size scaling are rather suppressed. Actually, as first noted by Ref. [17], the fidelity susceptibility detects the underlying singularity clearly out of the subdominant contributions. Last, a key ingredient is that χ_F 's singularity $\alpha_F/\nu = 0.9775$ [Eq. (9)] is substantially larger than that of the specific heat, $\alpha/\nu = -0.0225$ [36]; actually, the latter takes a negative value as for the 3D- XY universality. In this sense, the former is appropriate as a quantifier for the criticality.

2.3. Crossover-scaling plot of the fidelity susceptibility around $\eta = 0$: Analysis of the crossover exponent ϕ

We then turn to the analysis of the multicriticality at $\eta = 0$. For that purpose, we extend the above scaling formalism (7) to the crossover-scaling formula [28, 29]

$$\chi_F = L^{\dot{\alpha}_F/\dot{\nu}} g\left((H - H_c(\eta))L^{1/\dot{\nu}}, \eta L^{\phi/\dot{\nu}}\right), \quad (10)$$

with yet another controllable parameter η , the accompanying crossover exponent ϕ , and a scaling function g . Here, the indices, $\dot{\alpha}_F$ and $\dot{\nu}$, denote the fidelity-susceptibility and correlation-length critical exponents, respectively, right at the multicritical point $\eta = 0$. The meaning of the second argument of the crossover-scaling formula (10), $\eta L^{\phi/\dot{\nu}}$, is as follows. The correlation-length critical exponent $\dot{\nu}$ describes the singularity of the length scale L as $L \sim |H - H_c(0)|^{-\dot{\nu}}$. This relation leads to the physically convincing expression $\eta L^{\phi/\dot{\nu}} \sim \eta/|H - H_c(0)|^\phi$. Now, it is apparent that the crossover exponent ϕ describes the mutual relationship between H and the new entity η .

Before carrying out the crossover-scaling analyses, we fix the values of the critical indices appearing in the formula (10). As mentioned in Introduction, the phase transition along the ordinate axis $\eta = 0$ is essentially the same as that of the magnetization plateau, and the power-law singularities have been investigated in considerable detail [12] as follows. The correlation-length critical exponent was determined as $\dot{\nu} = 1/2$ [12, 38, 39]. This index immediately yields $\dot{\alpha}_F/\dot{\nu} = 3$ via the scaling relation $\dot{\alpha}_F/\dot{\nu} = \dot{\alpha}/\dot{\nu} + z$ [20]. Here, the dynamical critical exponent takes the value $z = 2$ [12], and the specific-heat critical exponent $\dot{\alpha} = 1/2$ comes from the idea that the field-induced magnetization, $\sim \sqrt{H - H_c}$ [12], is regarded as the internal energy. (Note that the first derivative of the ground-state energy corresponds to the ‘‘internal energy’’ in the classical statistical mechanical context.) The above consideration now completes the prerequisite for the crossover-scaling analysis. The remaining index ϕ is to be adjusted so as to achieve an alignment of the crossover-scaled χ_F data.

In Fig. 6, we present the crossover-scaling plot, $(H - H_c(\eta))L^{1/\dot{\nu}}\chi_F L^{-\dot{\alpha}_F/\dot{\nu}}$, for various system sizes, (+) $L = 3$, (\times) 4, and ($*$) 5, with $\dot{\nu} = 1/2$ and $\dot{\alpha}_F/\dot{\nu} = 3$ determined above. Here, we fixed the second argument of the scaling formula (10) to a constant value $\eta L^{\phi/\dot{\nu}} = 5$ with an optimal crossover exponent $\phi = 0.8$, and the parameter $H_c(\eta)$ was determined via the same scheme as that of Sec. 2.1. From Fig. 6, we see that the crossover-scaled data fall into the scaling curve satisfactorily. Particularly, the $L = 4$ (\times) and 5 ($*$) data are about to overlap each other. Such a feature suggests that the choice $\phi = 0.8$ is a feasible one.

Likewise, setting the crossover exponent to $\phi = 0.7$, in Fig. 7, we present the crossover-scaling plot, $(H - H_c(\eta))L^2\chi_F L^{-3}$, for various system sizes $L = 3, 4, 5$; the symbols are the same as those of Fig. 6. Here, the second argument of the crossover-scaling formula (10) is fixed to $\eta L^{2\phi} = 3.62$ with a proposition $\phi = 0.7$. For such a small value of $\phi = 0.7$, the crossover-scaled data get scattered; particularly, the left-side slope becomes dispersed, as compared to that of Fig. 6. Similarly, under the setting $\phi = 0.9$, in Fig. 8, we present the crossover-scaling plot, $(H - H_c(\eta))L^2\chi_F L^{-3}$, for various system sizes $L = 3, 4, 5$; the symbols are the same as those of Fig. 6. Here, the second argument of the crossover-scaling formula is set to a constant value $\eta L^{2\phi} = 6.9$ with $\phi = 0.9$. For such a large value of $\phi = 0.9$, the crossover-scaled data become scattered; actually, the hill-top data split up. Considering that the above cases, Figs. 7 and 8, yield the lower and upper bounds, respectively, for the estimate of ϕ , we conclude that the crossover exponent lies within

$$\phi = 0.8(1). \tag{11}$$

Our result excludes the possibility that the phase boundary $H_c(\eta)$ rises up linearly $\phi \approx 1$, as observed for the XY (namely, easy-plane $SU(2)$) magnet [8, 9, 10]. Rather, as for the extended internal symmetry group, the phase boundary is curved convexly, accompanying with a slightly suppressed crossover exponent (11).

A number of remarks are in order. First, the underlying physics behind the crossover-scaling plot, Fig. 6, differs from that of the fixed- η scaling, Fig. 5. Actually, the former scaling dimension $\dot{\alpha}_F/\dot{\nu} = 3$ is much larger than that of the latter, $\alpha_F/\nu = 0.9775$ [Eq. (9)]. Therefore, the index ϕ has to be adjusted carefully, and the collapse of the crossover-scaled data points, Fig. 6, is by no means coincidental. In this sense, the present crossover-scaling analysis captures the characteristics of the multicritical behavior. Second, because the fidelity-susceptibility approach does not rely on any presumptions as to the order parameter involved, it detects both singularities, $\dot{\alpha}/\dot{\nu} = 3$ and $\alpha/\nu = 0.9775$ [Eq. (9)], in a unified manner. Moreover, as mentioned in Sec. 2.2, the fidelity susceptibility is less affected by corrections to scaling [17], and it picks up the underlying singularity out of the subdominant contributions. Last, as explained in Introduction, so far, only the extremum cases, namely, the large- N [9] and easy-plane- $SU(2)$ [8, 9, 10] symmetry groups, have been considered, and the multicritical behavior in between remains unclear. Our result $\phi = 0.8(1)(< 1)$ [Eq. (11)] indicates that the phase boundary $H_c(\eta)$ is curved convexly, as the internal symmetry group

is extended to the easy-plane $SU(3)$. Because the reentrant behavior occurs only in $1 < d \leq 2.065\dots$ dimensions even for the large- N case [9], it is reasonable that the *slightly* enlarged $SU(3)$ group does not lead to the reentrant behavior immediately in $d = 2$ dimensions.

3. Summary and discussions

The two-dimensional easy-plane $SU(3)$ magnet under the transverse field (2) was investigated with the exact-diagonalization method. Because the method allows direct access to the ground state, we do not have to care about the anisotropy between the real-space and imaginary-time directions rendered by the dynamical critical exponent $z = 2(\neq 1)$ [12] at the multicritical point $\eta = 0$. Our main concern is to reconcile the discrepancy between the large- N theory [9] and the exact-diagonalization analysis of the XY magnet [8, 9, 10] as to the multicriticality (Fig. 2). For that purpose, we consider the $SU(3)$ version of the easy-plane magnet (2), and performed the exact-diagonalization simulation by the agency of the fidelity susceptibility χ_F (4). The fidelity susceptibility has an advantage in that it detects the phase transition sensitively, as compared to that of the specific heat [17, 20]. As a preliminary survey, setting the anisotropy parameter to $\eta = 1$, we estimate the critical point via χ_F as $H_c(1) = 6.53(5)$ [Eq. (6)]. This result is comparable to the preceding results, 6.300 [30], 6.628 [31, 32], and 6.524(23) [33], estimated with the BMFA, SCHA, and QMC methods, respectively. Particularly, our result $H_c(1) = 6.53(5)$ agrees with the large-scale-QMC-simulation result 6.524(23) [33], validating the χ_F -mediated simulation scheme. Thereby, we cast the χ_F data into the crossover-scaling formula (10) with the anisotropy η scaled properly. Adjusting the crossover exponent ϕ carefully, we attain an alignment of the crossover-scaled data points for $\phi = 0.8(1)$ [Eq. (11)]. This result $\phi < 1$ indicates that the phase boundary $H_c(\eta)$ gets curved convexly around the multicritical point $\eta = 0$, as the internal symmetry group is extended to $SU(3)$. Actually, only in $1 < d \leq 2.065\dots$ dimensions, the reentrant behavior is realized even for the large- N case [9]. Hence, it is reasonable that the slightly enlarged internal symmetry does not lead to the reentrant behavior immediately.

We conjecture that the phase boundary may exhibit a quadratic curvature, $\phi = 0.5$, eventually for an extremely large internal symmetry group, and above this threshold, the reentrant behavior should set in. It is thus tempting to consider the fractional-dimensional ($1 < d < 2$) system realized effectively by the power-law-decaying interactions [40]. In such a fractional-dimensional system, the reentrant behavior may come out even for the XY model. This problem is left for the future study.

Acknowledgments

This work was supported by a Grant-in-Aid for Scientific Research (C) from Japan Society for the Promotion of Science (Grant No. 20K03767).

Table 1. A number of preceding results for the critical point $H_c(1)$ at $\eta = 1$ are recollected. At $\eta = 1$, the model (2) reduces to the spin- $S = 1$ XY model with the single-ion anisotropy D . These D -based results are converted so as to match our notation via the relation $H = 2D/\sqrt{3}$. So far, a variety of techniques, such as the bosonic mean-field approximation (BMFA) [30], self-consistent harmonic approximation (SCHA) [31, 32], and quantum Monte Carlo (QMC) [33] methods, have been employed, and these results are comparable to the present exact diagonalization (ED) result. (The BMFA estimate is read off from Fig. 1 of Ref. [30].) In the respective studies, as a probe to detect the phase transition, various quantifiers, such as the spontaneous magnetization, energy gap, correlation length and fidelity susceptibility, were utilized. Because “the anisotropy does not have large effects” [30], the large-scale QMC result [33] for the Heisenberg model [34, 35] is shown as well.

Method	Quantifier	Model	$H_c(\eta = 1)$
BMFA [30]	spontaneous magnetization	XY	6.300
SCHA [31, 32]	energy gap	XY	6.628
QMC [33]	correlation length	Heisenberg	6.524(23)
ED (this work)	fidelity susceptibility	XY	6.53(5)

Appendix A. Transition point $H_c = 8/\sqrt{3}$ at $\eta = 0$

At the isotropic point $\eta = 0$, the location of the multicritical point $H_c(0) = 8/\sqrt{3}$ is obtained analytically as follows. For sufficiently large H , the ground state is given by the direct product $\otimes_i^N |0\rangle_i$ of the local base $|0\rangle_i$, which satisfies $S_i^z |m\rangle_i = m |m\rangle_i$ ($m = -1, 0, 1$) at each site i . Due to the strict selection rule at $\eta = 0$, magnons’ pair creation is prohibited. Thus, the single magnon at site j , $|j\rangle = |1\rangle_j \otimes (\otimes_{i \neq j}^N |0\rangle_i)$, propagates coherently through the transfer amplitude $-2J$ over the nearest neighbors, obeying the dispersion relation $-4J(\cos k_x + \cos k_y) + \sqrt{3}H$ (\mathbf{k} : wave number) above the ground state. Therefore, at $H_c(\eta = 0) = 8/\sqrt{3}$, the band gap closes in a way reminiscent of the metal-insulator transition. This transition mechanism is precisely the same as that of the magnetization plateau [12] (saturation of the magnetization). A notable point is that the dynamical critical exponent takes $z = 2$, because the *quadratic* band bottom touches the ground-state energy level. In other words, the symmetry between the real-space and imaginary-time directions is violated by $z \neq 1$. It is a benefit of the exact-diagonalization method that the method allows direct access to the ground state, for which the imaginary-time system size is infinite.

References

- [1] J. Maziero, H. C. Guzman, L. C. Céleri, M. S. Sarandy, and R. M. Serra, Phys. Rev. A **82** (2010) 012106.
- [2] Z.-Y. Sun, Y.-Y. Wu, J. Xu, H.-L. Huang, B.-F. Zhan, B. Wang, and C.-B. Duan, Phys. Rev. A **89** (2014) 022101.
- [3] G. Karpat, B. Çakmak, and F. F. Fanchini, Phys. Rev. B **90** (2014) 104431.

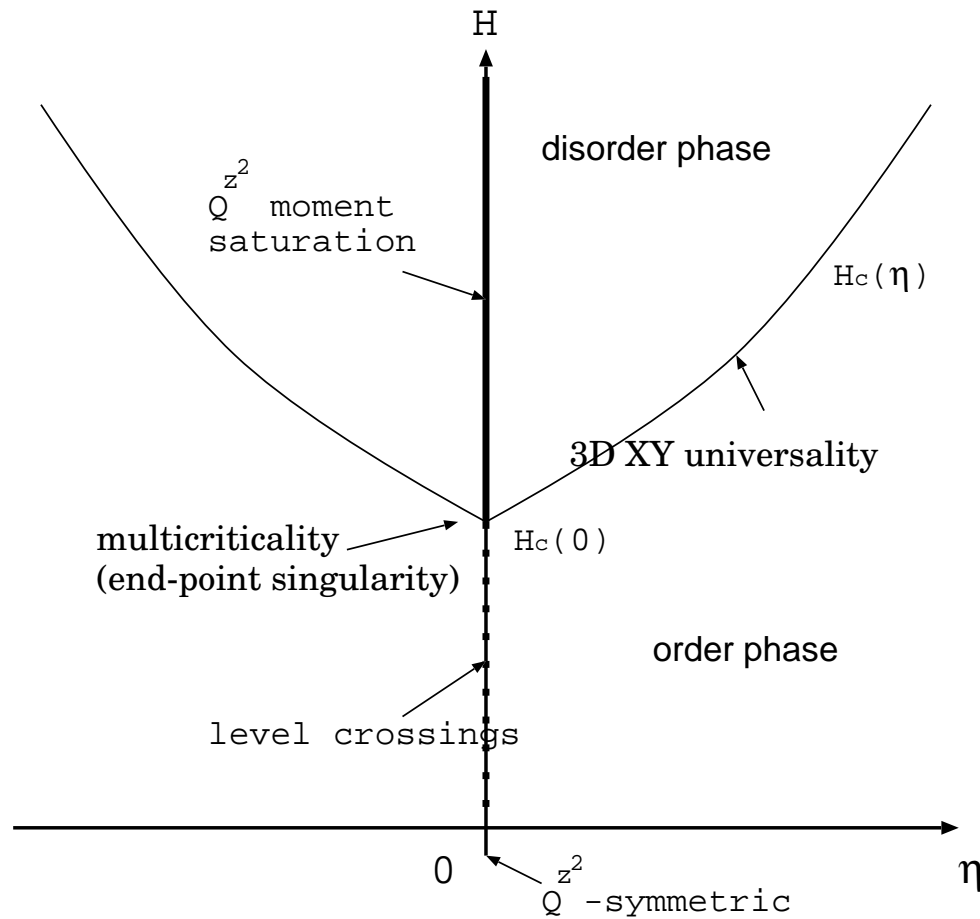


Figure 1. A schematic phase diagram of the easy-plane $SU(3)$ magnet (2) for the anisotropy η and transverse field H is presented. The phase boundary $H_c(\eta)$ terminates at the multicritical point $H = H_c(\eta = 0) = 8/\sqrt{3}$ at $\eta = 0$, and this end-point singularity is our concern. For small $H < H_c(\eta)$, the in-plane order, (S_i^x, S_i^y) $[(Q_i^{yz}, Q_i^{zx})]$ develops in the $\eta > (<)0$ side, whereas for large $H > H_c(\eta)$, the disorder phase extends. At the isotropic point $\eta = 0$ in between, the transverse moment $\sum_{i=1}^N Q_i^{z^2}$ commutes with the Hamiltonian, and the ground-state level crossing occurs successively [7] up to $H < H_c(0)$. Above this threshold $H > H_c(0)$, the magnetization plateau [12] (saturation of the moment $\sum_{i=1}^N Q_i^{z^2}$) sets in.

- [4] Q. Luo, J. Zhao, and X. Wang, Phys. Rev. E **98** (2018) 022106.
- [5] A. Steane, Rep. Prog. Phys. **61** (1998) 117.
- [6] C.H. Bennett and D.P. DiVincenzo, Nature **404** (2000) 247.
- [7] V. Mukherjee, A. Polkovnikov, and A. Dutta, Phys. Rev. B **83** (2011) 075118.
- [8] M. Henkel, J. Phys. A: Mathematical and Theoretical **17** (1984) L795.
- [9] S. Wald and M. Henkel, J. Stat. Mech.: Theory and Experiment (2015) P07006.
- [10] Y. Nishiyama, Eur. Phys. J. B **92** (2019) 167.
- [11] S. Jalal, R. Khare, and S. Lal, arXiv:1610.09845.
- [12] V. Zapf, M. Jaime, and C. D. Batista, Rev. Mod. Phys. **86** (2014) 563.
- [13] J. D’Emidio and R. K. Kaul, Phys. Rev. B **93** (2016) 054406.
- [14] H. T. Quan, Z. Song, X. F. Liu, P. Zanardi, and C. P. Sun, Phys. Rev. Lett. **96** (2006) 140604.
- [15] P. Zanardi and N. Paunković, Phys. Rev. E **74** (2006) 031123.
- [16] H.-Q. Zhou, and J. P. Barjaktarevič, J. Phys. A: Math. Theor. **41** (2008) 412001.

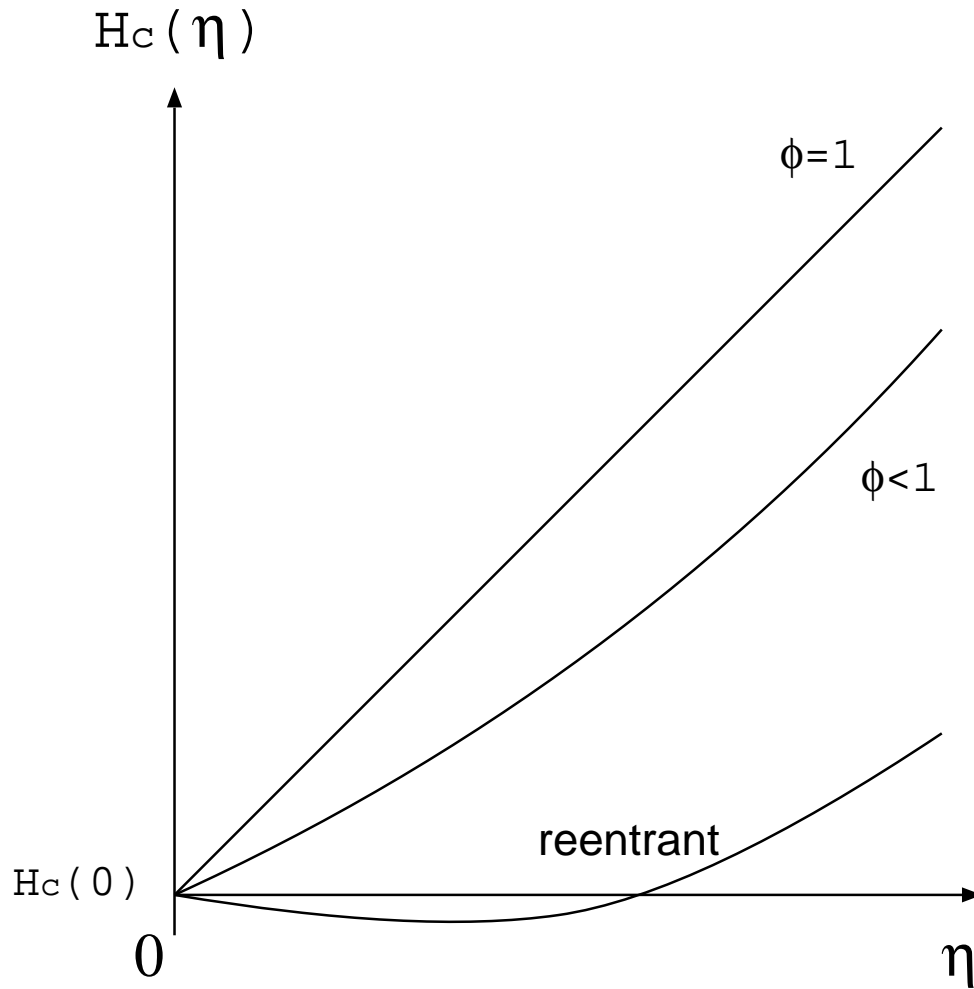


Figure 2. The multicriticality (end-point singularity) of the phase boundary $H_c(\eta)$ at $\eta = 0$ is characterized by the crossover exponent ϕ [28, 29] such as $H_c(\eta) - H_c(0) \sim |\eta|^{1/\phi}$ (3). As for the XY model (namely, the easy-plane $SU(2)$ magnet), the exact-diagonalization simulation suggests that the phase boundary rises up linearly with $\phi \approx 1$ [8, 9, 10]. On the one hand, the large- N analysis admits the reentrant (non-monotonic) behavior [9]. As indicated, the reentrant behavior leads to a counterintuitive picture such that the disorder phase is induced by the lower internal symmetry group $\eta \neq 0$ around the multicritical point. It is anticipated that for the $SU(3)$ case, the phase boundary is curved convexly with a slightly suppressed crossover exponent $\phi < 1$.

- [17] W.-C. Yu, H.-M. Kwok, J. Cao and S.-J. Gu, Phys. Rev. E **80** (2009) 021108.
- [18] W.-L. You and Y.-L. Dong, Phys. Rev. B **84** (2011) 174426.
- [19] D. Rossini and E. Vicari, Phys. Rev. E **98** (2018) 062137.
- [20] A. F. Albuquerque, F. Alet, C. Sire, and S. Capponi, Phys. Rev. B **81** (2010) 064418.
- [21] D. Schwandt, F. Alet, and S. Capponi, Phys. Rev. Lett. **103** (2009) 170501.
- [22] A. Uhlmann, Rep. Math. Phys. **9** (1976) 273.
- [23] R. Jozsa, J. Mod. Opt. **41** (1994) 2315.
- [24] A. Peres, Phys. Rev. A **30** (1984) 1610.
- [25] T. Gorin, T. Prosen, T. H. Seligman, and M. Žnidarič, Phys. Rep. **435** (2006) 33.

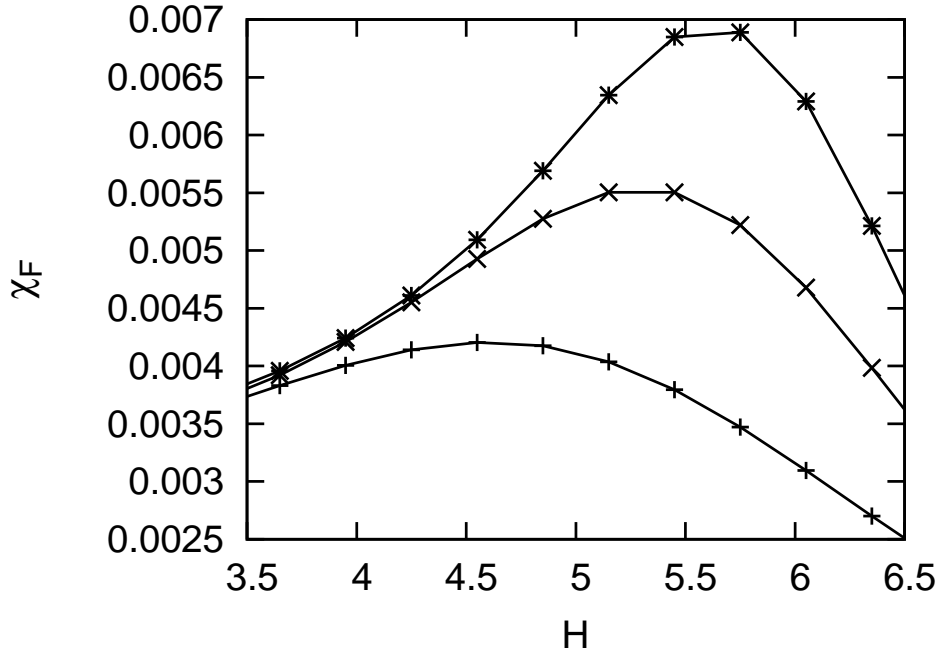


Figure 3. The fidelity susceptibility χ_F (4) is plotted for various values of the transverse field H and the system sizes, (+) $L = 3$, (\times) 4, and ($*$) 5, with the fixed anisotropy parameter $\eta = 1$. The fidelity susceptibility indicates a notable peak around the critical point $H \approx 6$.

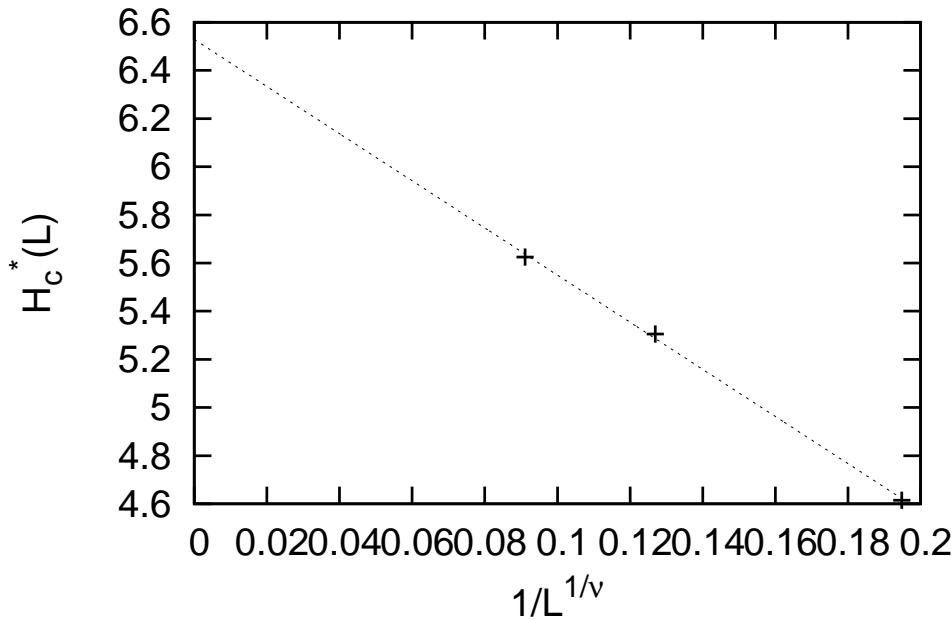


Figure 4. The approximate critical point $H_c^*(L)$ (5) is plotted for $1/L^{1/\nu}$ with the fixed anisotropy parameter $\eta = 1$. Here, the correlation-length critical exponent is set to the 3D-XY-universality value $\nu = 0.6717$ [36, 37]. The least-squares fit to these data yields an estimate $H_c = 6.53(5)$ in the thermodynamic limit $L \rightarrow \infty$.

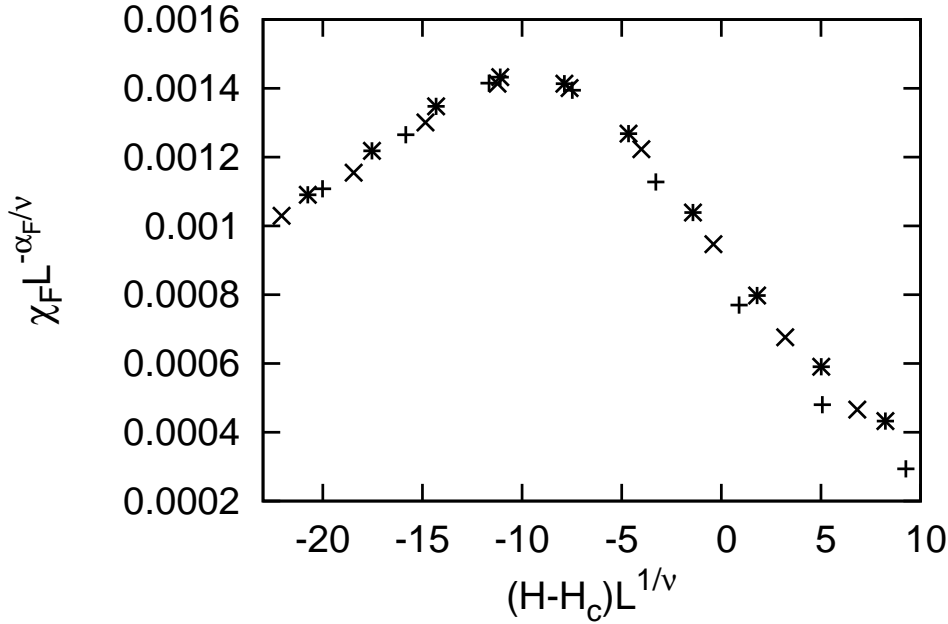


Figure 5. The scaling plot, $(H - H_c)L^{1/\nu} - \chi_{FL} L^{-\alpha_F/\nu}$, is presented for various system sizes, (+) $L = 3$, (\times) $L = 4$, and ($*$) $L = 5$, with the fixed $\eta = 1$; see the scaling formula (7). Here, the scaling parameters are set to $H_c = 6.53$ [Eq. (6)], $\nu = 0.6717$ [36, 37] and $\alpha_F/\nu = 0.9775$ [Eq. (9)]. The scaled data collapse into the scaling curve satisfactorily, suggesting that the criticality belongs to the 3D-XY universality class.

- [26] A. Läuchli, F. Mila, and K. Penc, Phys. Rev. Lett. **97** (2006) 087205.
- [27] V. Z. Kashurnikov, N. V. Prokof'ev, B. V. Scistunov, and M. Troyer, Phys. Rev. B **59** (1999) 1162.
- [28] E.K. Riedel and F. Wegner, Z. Phys. **225** (1969) 195.
- [29] P. Pfeuty, D. Jasnow, and M. E. Fisher, Phys. Rev. B **10** (1974) 2088.
- [30] H.-T. Wang and Y. Wang, Phys. Rev. B **71** (2005) 104429.
- [31] A.S.T. Pires, J. Mag. Mag. Mat. **323** (2011) 1977.
- [32] A.R. Moura, J. Mag. Mag. Mat. **369** (2014) 62.
- [33] T. Roscilde and S. Haas, Phys. Rev. Lett. **99** (2007) 047205.
- [34] C. J. Hamer, O. Rojas, and J. Oitmaa, Phys. Rev. B **81** (2010) 214424.
- [35] Z. Zhang, K. Wierschem, I. Yap, Y. Kato, C. D. Batista, and P. Sengupta, Phys. Rev. B **87** (2013) 174405.
- [36] M. Campostrini, M. Hasenbusch, A. Pelissetto, and E. Vicari, Phys. Rev. B **74**, 144506 (2006).
- [37] E. Burovski, J. Machta, N. Prokof'ev, and B. Svistunov, Phys. Rev. B **74**, 132502 (2006).
- [38] M. Adamski, J. Jędrzejewski, and T. Krokhamalskii, arXiv:1502.05268.
- [39] C. Hoeger, G. V. Gehlen, and V. Rittenberg, J. Phys. A: Math. Gen. **18** (1985) 1813.
- [40] N. Defenu, A. Trombettoni, and S. Ruffo, Phys. Rev. B **96** (2017) 104432.

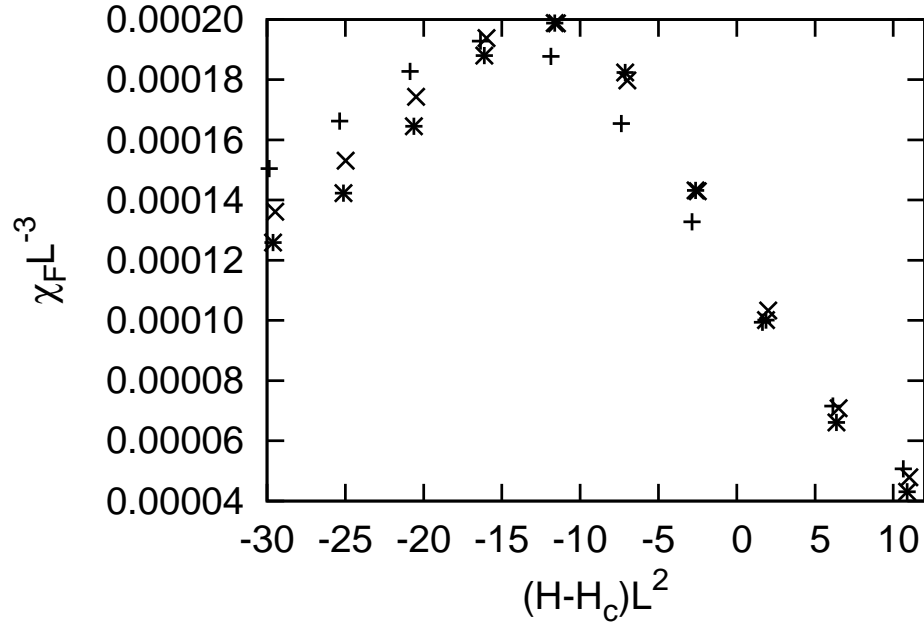


Figure 6. The crossover-scaling plot, $(H - H_c(\eta))L^{1/\nu} - \chi_{FL}^{-\alpha_F/\nu}$, is presented for various system sizes, (+) $L = 3$, (\times) $L = 4$, and ($*$) $L = 5$, with $\nu = 1/2$ [12] and $\alpha_F/\nu = 3$; see text for details. Here, the second argument of the crossover-scaling formula (10) is fixed to $\eta L^{\phi/\nu} = 5$ with the crossover exponent $\phi = 0.8$. The crossover-scaled data fall into the scaling curve satisfactorily; particularly, the $L = 4$ (\times) and $L = 5$ ($*$) data are about to overlap each other under the setting, $\phi = 0.8$.

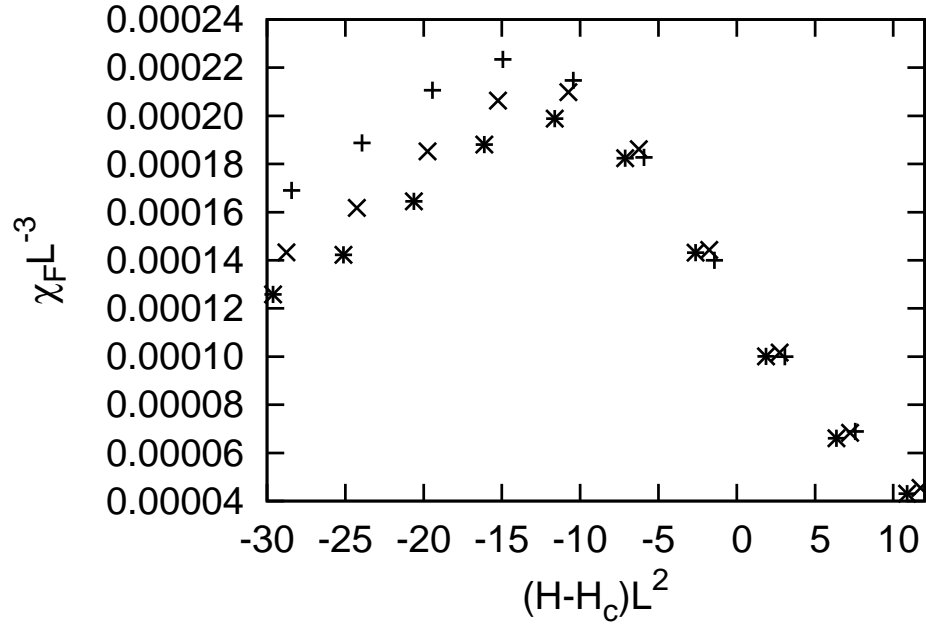


Figure 7. The crossover-scaling plot, $(H - H_c(\eta))L^{1/\nu} - \chi_{FL}^{-\alpha_F/\nu}$, is presented for various system sizes, (+) $L = 3$, (x) $L = 4$, and (*) $L = 5$, with $\nu = 1/2$ and $\alpha_F/\nu = 3$. Here, the second argument of the crossover-scaling formula (10) is fixed to $\eta L^{\phi/\nu} = 3.62$ with the crossover exponent $\phi = 0.7$. The left-side slope gets scattered under such a small value of $\phi = 0.7$.

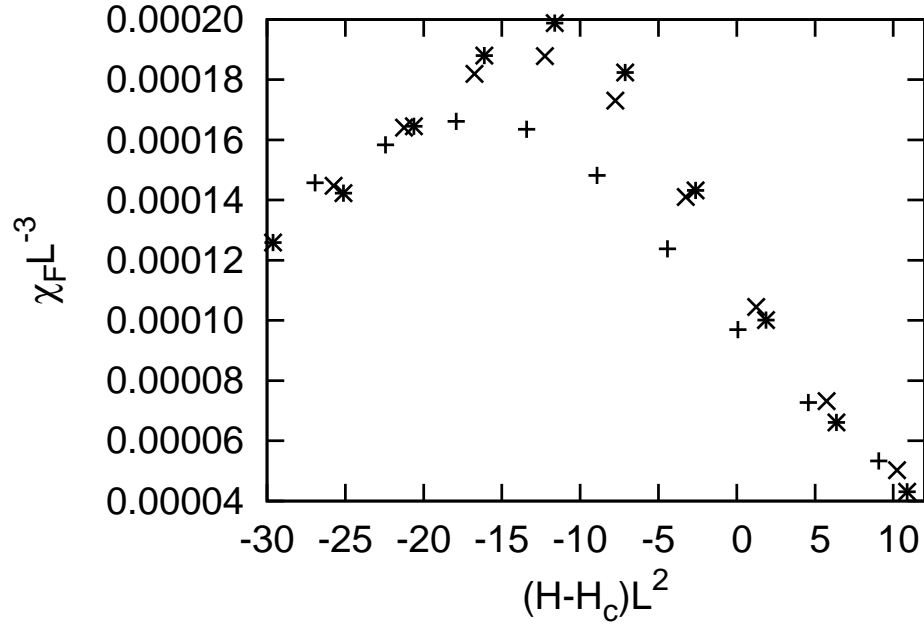


Figure 8. The crossover-scaling plot, $(H - H_c(\eta))L^{1/\nu} - \chi_{FL}^{-\alpha_F/\nu}$, is presented for various system sizes, (+) $L = 3$, (\times) 4 , and ($*$) 5 , with $\nu = 1/2$ and $\alpha_F/\nu = 3$. Here, the second argument of the crossover-scaling formula (10) is fixed to $\eta L^{\phi/\nu} = 6.9$ with the crossover exponent $\phi = 0.9$. The hill-top data split up for such a large value of $\phi = 0.9$.